Article

Fast detection of 2,4,6-trinitrotoluene (TNT) at ppt level by an immunosensor based on kinetic competition

Martin Paul [ORCID], Georg Tscheuschner [ORCID], Stefan Herrmann [ORCID], Michael G. Weller [ORCID]*

Federal Institute for Materials Research and Testing (BAM), Division 1.5 Protein Analysis, Richard-Willstätter-Strasse 11, 12489 Berlin, Germany

* Correspondence: michael.weller@bam.de; Tel.: +49-30-8104-1150

Abstract: The illegal use of explosives by terrorists and other criminals is an increasing issue in public spaces, such as airports, railway stations, highways, sports arenas, theaters, and other large buildings. Security in these environments can be achieved by a set of different means, including the installation of scanners and other analytical devices to detect ultra-small traces of explosives in a very short time-frame to be able to take action as early as possible to prevent the detonation of such devices. Unfortunately, an ideal explosive detection system still does not exist, which means that a compromise is needed in practice. Most detection devices lack the extreme analytical sensitivity, which is nevertheless necessary due to the low vapor pressure of nearly all explosives. In addition, the rate of false positives needs to be virtually zero, which is also very difficult to achieve. Here we present an immunosensor system based on kinetic competition, which is known to be very fast and may even overcome affinity limitation, which impairs the performance of many traditional competitive assays. This immunosensor consists of a monolithic glass column with a vast excess of immobilized hapten, which traps the fluorescently labeled antibody as long as no explosive is present. In the case of TNT occurring, some binding sites of the antibody will be blocked, which leads to an immediate breakthrough of the labeled protein, detectable by highly sensitive laser-induced fluorescence with the help of a Peltier-cooled CMOS camera. Liquid handling is performed with high-precision syringe pumps and chip-based mixing-devices and flow-cells. The system achieved limits of detection of 1 pM (1 ppt) of the fluorescent label and around 100 pM (20 ppt) of the explosive 2,4,6-trinitrotoluene (TNT). The total assay time is less than 8 min. A cross-reactivity test with 5000 pM solutions showed no signal by PETN, RDX, and HMX. This immunosensor belongs to the most sensitive and fastest detectors for TNT with no significant cross-reactivity by non-related compounds.

Keywords: Aviation security; biosensor; flow injection assay; monoclonal antibody; fluorescence microscope; lab-on-a-chip; microfluidic systems; antibody labeling; CMOS; diode laser; monolithic column; laser-induced fluorescence detector (LIF).

1. Introduction

The fast and extremely sensitive detection of explosives [1-3] is one of the most relevant tasks to guarantee security in areas of public access. Many airplane passengers are confronted with some security measures, from which the ban of most liquids in the luggage is one of the least popular. X-ray-based scanners are used in most airports, which may detect larger amounts of explosives. However, for trace analysis, additional wipe tests may be necessary. Nevertheless, the ultimate explosive detector is still the dog, which is requested in nearly all critical situations. Considering the high cost of a trained animal with its handler and the inability to use them for extended missions, it becomes clear that an automated sensor system would be highly desirable. The first steps towards an electronic dog nose were published some time ago [4]. Unfortunately, no sensor system can compete

Peer-reviewed version available at Biosensors 2020, 10, 89; doi:10.3390/bios10080089

with dogs and other animals, yet. In addition, the most powerful instrumental analysis systems are not mobile and are limited to a laboratory environment.

Up to now, several sensor systems have been developed to detect traces of explosives. Perhaps the most well-known devices are based on Ion Mobility Spectrometry (IMS) [5], which are commercially available and claim sensitivities down to ppb. However, sensitivity and particularly selectivity still need to be improved [6], since false positive from household products seem to be common. Quite a few chemosensors have been presented [7], which are often based on quartz microbalances [8,9] or fluorescence quenching, e.g. [10-18]. Many sensors of the latter type display stunning sensitivity, which may explain their popularity in the research field. Unfortunately, most publications show only very sparse cross-reactivity data. In addition, the transfer of these systems to other explosives, such as PETN or TATP, seems to be generally difficult, if not impossible.

A review of different luminescence-based methods was published in 2008 [19]. In the same year, a review of biosensors and bioinspired systems appeared [20]. In this article, not only antibody-based methods were mentioned, but also systems using aptamers, peptides [21], cyclodextrins, MIPs [22-24], odorant-binding proteins, bacteria, algae, and yeasts. A particularly interesting concept is the combination of molecularly imprinted polymers (MIPs) with fluorescence, which combines the selectivity of MIPs with the sensitivity of fluorescence detection [25]. Furthermore, immunosensors have been examined for a while [26-36]. Some of them are based on surface plasmon resonance technology (SPR) [37,38]. Others used antibody-gated mesoporous silica nanoparticles [39]. Also, electrochemical immunosensors have been developed [40,41]. They often showed promising performance parameters. Unfortunately, not many antibodies against explosives are available, although some had been developed and characterized [42-52]. However, their broader development seems to have stalled for some time.

For the fast and sensitive detection of explosives with antibodies, kinetic immunoassays are promising. This concept has first been presented in 1984 by Freytag et al. [53-55]. Later these assay types were varied and discussed in more detail [56-66]. Unfortunately, the nomenclature for these assays is quite diverse. To the best of our knowledge, this approach has never been used for security applications before. A somehow related format is known as kinetic exclusion assay [67,68], which, however, detects the bound receptor molecules and not the eluted fraction.

In our format, a labeled high-affinity antibody is mixed, preincubated with the sample, and passed through a hapten-coated affinity column. A fluorescent antibody with free binding sites can bind to the affinity column, while antibodies with binding sites blocked by analyte molecules would not be retained, instantly elute from the column, and are detected in a sensitive fluorescence detector (Fig. 1).

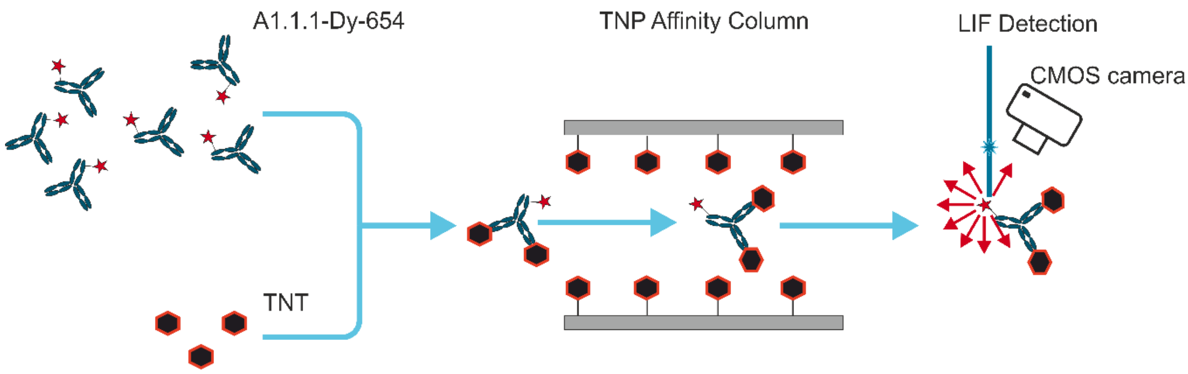

Figure 1. Kinetic competition biosensor: Labelled antibody is preincubated with the sample and pumped through the antigen-coated affinity column: The eluate passes a sensitive, laser-induced fluorescence detector (LIF).

As antibody binding is a reversible process, antibodies with off rates far longer than the column passage time are required to allow sensitive detection of the analyte. This means that high-affinity antibodies are needed for optimal assay performance. Furthermore, inactive antibodies would contribute to the background of this assay. Hence, highly purified antibody conjugates are preferable.

2. Materials and Methods

2.1. Reagents, buffers, materials, and equipment

Transparent, flat-bottom high binding 96-well microtiter plates (655101) were acquired from Greiner Bio-One (Frickenhausen, Germany), PD SpinTrap™ G-25 Desalting Columns (28918004) were obtained from GE Healthcare (Uppsala, Sweden), monoclonal anti-TNT antibody A1.1.1 [45] was obtained from SDIX (Newark, USA), goat anti-mouse HRP-conjugated antibody (15-035-003) was obtained from Jackson immune research (Cambridge, UK), fluorescence dye Dy-654-NHS and Dy-654-COOH were purchased from Dyomics (Jena, Germany). According to the manufacturer, the following properties of the dye Dy-654 are given: Excitation/emission max. 653/677 nm (in ethanol), molar absorbance: 220.000 $M^{-1}cm^{-1}$, soluble in water, methanol, and DMF (https://dyomics.com/en/products/red-excitation/dy-654). Bovine serum albumin >98% (BSA, A7906), diethoxy(3-glycidyloxypropyl)-methyl silane (539252), Mucasol (Z637203), ProClin300 (8912-U) and 5% (w/v) picrylsulfonic acid solution (TNBS, P2297) were purchased from Sigma-Aldrich (Taufkirchen, Germany). Hydrochloric acid (HCl, 84415) was purchased from Fluka, and cyano-4-hydroxycinnamic acid (CHCA) was bought from Bruker Daltonics (Bremen, Germany), sodium bicarbonate (1940) and potassium hydroxide (121515) were obtained from AppliChem (Darmstadt, Germany), TMB substrate (SeramunBlau fast2) were bought from Seramun (Heidesee, Germany), Tween 20 (37470.01) was bought from Serva (Heidelberg, Germany), absolute ethanol (2246) from Th. Geyer (Renningen, Germany) and labeling grade DMF (13050) was bought from Lumiprobe (Hunt Valley, USA). 2,4,6-Trinitrotoluene (TNT), pentaerythritol tetranitrate (PETN), 1,3,5-trinitroperhydro-1,3,5-triazine (RDX), octahydro-1,3,5,7-tetranitro-1,3,5,7-tetrazocine (HMX) were kindly supplied by BAM Division 2.3. Vitrapor5 glass monoliths were acquired from ROBU (Hattert, Germany), and ultrapure water (MilliQ) was supplied by a Milli-Q Synthesis A10 system (Merck, Germany). The bandpass filter (FL635-10), the dichroic mirror (DMLP638R), the long pass filters (FELH650), and the tube lens (TTL165-A) were purchased from Thorlabs (Newton, USA). The objective plan achromat 10x/0,25 Ph1 (415500-1605-001) was obtained from Carl Zeiss (Oberkochen, Germany), the diode laser 70105582 from Picotronic (Koblenz, Germany), the microfluidic chip (10000091) from Microfluidic ChipShop (Jena, Germany), the injection valve (5067-4158) from Agilent (Santa Clara, USA) and a Fusion 4000 syringe pump was acquired from Chemyx (Stafford, USA). MALDI-TOF mass spectrometry was performed on a Bruker Autoflex II Smartbeam, and Autoflex Max MS and absorbance was measured with an Epoch2 photo spectrometer from Biotek (Vermont, USA). Data Evaluation was performed with Python 3.7 in Anaconda (Spyder 3.3.2) and Origin (2018G).

2.2. Trinitrophenyl-BSA conjugates and indirect competitive ELISA

Trinitrophenyl-(TNP)-BSA conjugate for the affinity column coating: In 1 mL of 0.2 M $NaHCO_3$ 20 mg (0.3 µM) of BSA was dissolved and 26.4 µl (4.5 µM) of 5 (w/v) % aqueous trinitrobenzene sulfonic acid (TNBS) was added, vortexed and stored for one hour at RT and subsequently for 48 h at 4 °C. After incubation, 125 µl of 2 M NaH_2PO_4 was added to adjust the solution to a neutral pH. A mean degree of labeling (DOL) of approx. 8 TNP per BSA was determined with MALDI-TOF MS (see Fig. S2)

TNP-BSA conjugate for indirect ELISA: In 5 mL of 0.2 M $NaHCO_3$ 100 mg (1.5 µM) of BSA were dissolved and 88 µl (15 µM) of TNBS (5%) were added, vortexed and stored for 1 h at RT and subsequently for 48 h at 4 °C. After incubation, 625 µl of 2 M NaH_2PO_4 was added to adjust the solution to a neutral pH. A DOL of 5 TNP per BSA was determined by MALDI-TOF MS (see Fig. S12).

Peer-reviewed version available at *Biosensors* **2020**, *10*, 89; doi:10.3390/bios10080089

ELISA procedure: Clear, high binding 96-well plates (MTP) with flat bottom were coated with 100 µl of a blend of 0.023 g/L TNP-BSA and 0.75 g/L BSA in PBS with 10 mM phosphate and 137 mM sodium chloride pH = 7.4 (100 µL per well). The plate was sealed with Parafilm, protected from light with aluminum foil and shaken at 750 rpm for 20 hours at RT. The MTP was washed three times, with PBS containing 0.05 % (v/v) Tween 20 by an automated plate washer.
Then 50 µl of diluted TNT in PBS ranging from 10 pM to 10 µM and 50 µl of 1:20 000 diluted A1.1.1-Dy-654 (approx. 17.5 µg/L) in PBS were added as quadruplicates and incubated for one hour at RT in the dark.
After a washing step, 100 µl of 40 µg/L HRP-conjugated anti-mouse (H+L) IgG antibody in PBS with 1 % BSA were incubated for one hour in the dark and the MTP was subsequently washed. Then 100 µl TMB substrate (Seramun Blau fast2) was incubated for 30 minutes and stopped with 100 µl of 0.25 M sulfuric acid. The absorbance was recorded with an Epoch2 Photometer at 450 and 620 nm.

2.3. Manufacturing of Affinity Columns

Cylindrical Vitrapor5 glass monoliths (15x8 mm) were glued into titanium shells (15x12 mm, wall thickness: 1 mm) with silicone glue and inserted into custom-designed and additively manufactured column holders with matching 1/16" threaded PEEK inlets (see Fig. S1).

The column was cleaned, and silanized with diethoxy(3-glycidyloxypropyl)-methyl silane, as described in Table T1 (Supplementary Information).

For the preparation of the TNP-BSA affinity column, 440 µl of the 7.8 eq. TNP-BSA solution was diluted with 2100 µl 0.1 M Na_2HPO_4 pH 8.1 and incubated for one week at RT on the epoxy-functionalized raw column.

2.4. Design and synthesis of the A1.1.1 fluorophore conjugate

In order to prepare the 4.54 mM Dy-654-NHS labeling solution, 0.2 mg of the NHS ester (0.18 µM) were dissolved in 40 µl of dry, amine-free DMF (labeling grade, Lumiprobe) and aliquoted to 10 µl portions and stored in the dark at – 18 °C.

To label the antibody, 9.18 µl (0.68 nM) of the A1.1.1 stock solution (10.9 g/L) in PBS containing 0.05 wt. % NaN_3 was diluted with 91 µl of PBS to 1 mg/L. A PD Spintrap G-25 was centrifuged dry for one minute at 800 g and 4°C and subsequently purged and centrifugated four times with 140 µl of 0.1 M Na_2HPO_4 and 1.37 M NaCl adjusted to pH 7.8. On the conditioned PD Spintrap, 100 µl of diluted antibody-solution and an additional 40 µl stacker volume of PBS were transferred and centrifuged at 800 g and 4°C for one minute, 140 µl of eluate were collected. The eluate, containing approx. 95 µg A1.1.1 (0.63 nM IgG), was cooled to 4 °C and six-fold access of label, 0.84 µl of the labeling solution (3.8 nM Dy-654-NHS) were added. The solutions were gently mixed by pipetting and incubated for 3 h at 14 °C in the dark and for 18 h in the dark at 4°C. The solution was purified with a PBS conditioned PD Spintrap G-25. The conjugate was stabilized with 0.04 % (v/v) ProClin300 and stored in the dark at 4°C.

2.5. Fluorescence detector

The custom detector based on an epifluorescence microscope setup was built from modular and affordable parts (see Table T2, Supplementary Information, SI), the detailed construction plans can be found in Fig. S4 (SI). As a detector, the camera QHY174M-GPS from QHYCCD (Beijing, China) was used, featuring an IMX-174M (Sony) CMOS sensor. This sensor is thermoelectrically cooled, has 5.86 x 5.86 µm square pixels, and delivers a maximal dynamic range of 12 bit. Data is acquired via a USB 3.0 connection by a laptop with the Software SharpCap (Version 3.0.4074.0).

In the excitation path (Figure 2, orange color), a diode laser (70105582, Picotronic) with a measured center-wavelength of 638 nm with a full width at half maximum (FWHM) of approx. 3 nm (see Fig. S7, SI) and an optical output power below 1 mW was used. The laser was directed through an FL635-10 bandpass filter and guided at 45° on a dichroic mirror (DMLP638R, THORLABS) with a

Preprints (www.preprints.org) | NOT PEER-REVIEWED | Posted: 3 July 2020 doi:10.20944/preprints202007.0039.v1

Peer-reviewed version available at Biosensors 2020, 10, 89; doi:10.3390/bios10080089

cutoff wavelength of 638 nm; the excitation was focused by an infinity-corrected plan achromat 10x/0,25 Ph1 objective (415500-1605-001, ZEISS) on a microfluidic COC (cyclic olefin copolymer) chip. The microfluidic chip (10000091, Microfluidic ChipShop) features four 200 x 200 µm linear flow channels and is mounted on a custom holder for precision adjustment (see Fig. S5, SI).

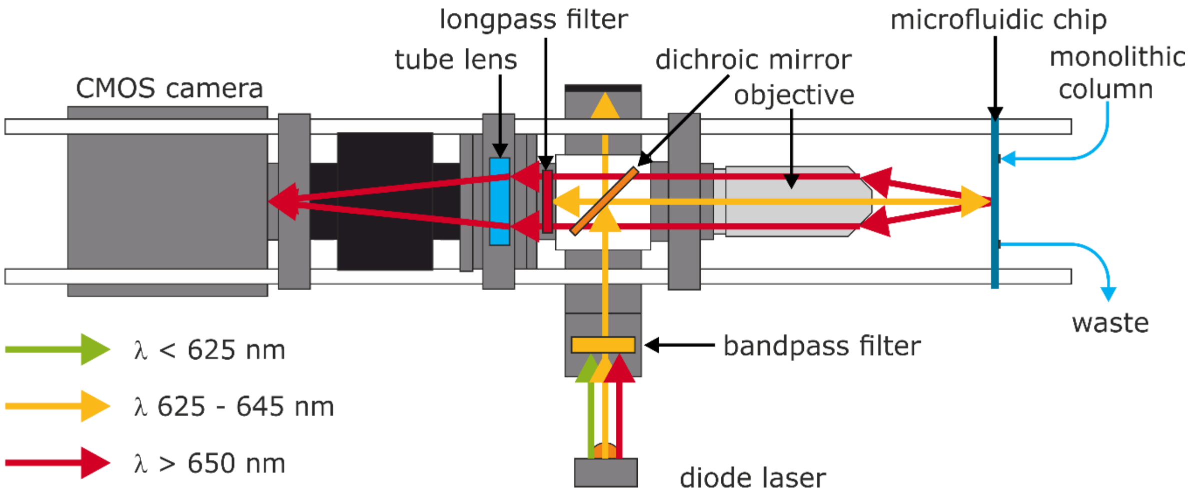

Figure 2. Light paths in the setup with important optical components.

In the fluorescence path (red), the fluorescence of the label in the flow channel is collected by the objective, filtered by two stacked long-pass filters (FELH650, THORLABS), and focused with an f 165 mm tube lens (TTl165-A, THORLABS) on the sensor of the camera(QHY174M-GPS, QHY). The whole setup is mounted on an optical breadboard and protected from environmental light and dust with a box made of black cardboard.

2.5. Measurements

All samples and buffers were injected with a Fusion 4000 dual syringe pump (Chemyx). The flow was directed to the column holder, which contained the monolithic column, and the eluate was subsequently passed through the flow channel of the microfluidic chip (see Fig. 2). In order to ensure bioinert conditions, all connectors were manufactured from PEEK or PP, and the sealings were made from silicone. The column holder was manufactured additively and had custom PEEK connectors; the columns may conveniently be exchanged (see Fig. S1). The typical backpressure of the monolithic column at a flow rate of 0.5 mL min^{-1} was approx. 2.7 bar (see Fig. S3). Therefore, the actual overall system pressure is low enough to operate the whole fluidics with standard plastic (PP) syringes and PTFE-silicone tubes. The total flow rates were capped to 0.5 mL min^{-1} as the microfluidic chip with the linear flow cell was limiting.

Setup of the sensitivity test: Dy-654-COOH was diluted to from 5 to 25 pM in 5 pM steps and from 100 to 1000 pM in 100 pM steps and injected with a 12 mL syringe with PBS blanks in between the samples. The data were recorded with an exposure time of 5,000 ms; the gain was set to four, and the sensor temperature was set to -5°C.
TNT detection: 2,4,6-trinitrotoluene (TNT) was diluted from a stock solution in ethanol to 0.4 to 2 nM in 0.4 nM steps and from 4 to 20 nM in 4 nm steps in PBS with 0.1 (w/v) % BSA and mixed 1:1 with A1.1.1-Dy-654 (1:50,000, approx. 7 µg/L) in PBS with 0.1 (w/v) % BSA, incubated for five minutes and injected through a six-way-valve as shown in Fig. 3. The data was recorded as described above.

Cross-reactivity tests: TNT, PETN, RDX, and HMX were diluted from a stock solution in methanol to 10 nM in PBS with 0.1 (w/v) % BSA and mixed 1:1 with diluted A1.1.1-Dy-654 (1:50,000, approx. 7 µg/L) in PBS with 0.1 (w/v) % BSA, incubated for five minutes and injected at a flow rate of 0.5 mL min^{-1} with six-way-valve as shown in Fig. 3. The data was recorded as described above.

Preprints (www.preprints.org) | NOT PEER-REVIEWED | Posted: 3 July 2020 doi:10.20944/preprints202007.0039.v1

Peer-reviewed version available at Biosensors 2020, 10, 89; doi:10.3390/bios10080089

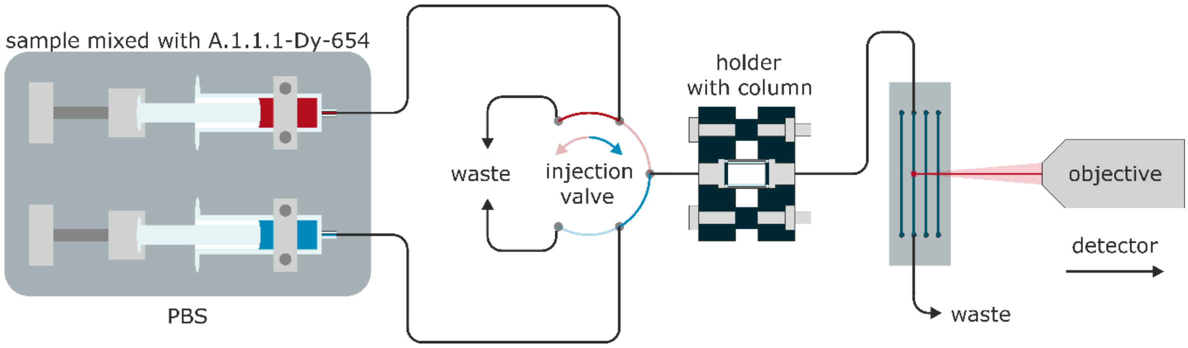

Figure 3. Microfluidic setup for the detection of TNT and the CR determination with six-way-valve for continuous flow injection.

3. Results

3.1. Fluorescence detector

The two stacked long-pass-filters and the dichroic mirror efficiently prevent stray light from the excitation laser with a center wavelength of 638 nm and an FWHM of approx. 3 nm to reach the sensor and allows for sensitive fluorescence detection. In preliminary experiments, the use of an additional second long-pass filter has proven to be beneficial. The microfluidic chip is made from TOPAS® (cyclic olefin copolymer, COC), which shows a very low autofluorescence at the used wavelength and has a smooth flat and transparent surface suitable for observation. The fluorescence is collected with the same 10X 0.25 NA objective and guided through the dichroic mirror and passed through the long-pass-filters. Overall a high transmission for the fluorescence is to be expected as the filters show high transmission of about 90% at 654 nm, which is the peak wavelength of Dy-654 emission. The monochromatic sensor of the QHY is reported to exhibit a high quantum yield of approx. 50% at 650 nm and is therefore suited for the application. The position of the excitation laser spot on the microfluidic chip can conveniently be adjusted by the additive manufactured laser holder (see Fig. S5) and is set in the center of the flow channel.

3.2. Semi-automated data evaluation with python

The images are recorded as a sequence of raw files (.fits) and have a native resolution of 1920 x 1080 pixels. The size of the laser-illuminated spot, which essentially defines the ROI (region of interest), is only a few pixels wide. Due to this small area, the exact position of the ROI in every frame is of high importance for the correct and reliable data evaluation. It was observed that within elongated measurement periods, the ROI position might be shifted slightly by a few pixels in x- and or y-direction. This behavior is most likely a result of the thermal expansion of the additive manufactured laser-holder (Fig. S5). In order to account for this shift, the correct position of the ROI must be determined automatically but precisely for every frame. By a semi-automated python-script, a Gaussian fit is utilized to determine the center pixel of the laser spot, based on which a pixel-square ROI is defined.

Around the determined laser center, a square ROI region of 8x8 pixels is created, and all 64 pixels inside are sorted by their intensity. The three most intense pixels are discarded to account for possible cosmic rays or hot pixels. Subsequently, the following five pixels are used to calculate the mean value, which is defined as intensity for the frame. To determine the signal intensity of an injected probe, for example, the 100 pM Dy-654-COOH solution, 16-frames are used to calculate the mean value and the standard deviation. To determine the starting point for the signal evaluation (f_n), the raw-signal is smoothed by a Savitzky–Golay filter with a polynomial of second-order and a window of five frames. Subsequently, the gradient of the smoothed data is calculated. The first sample point of the 1st derivative to fall below zero after the initial signal increase is picked (see Fig. 4) and defined as f_n, as it represents a stable signal as growth is completed. Based on this frame, f_n and the next 15 frames are used to calculate the mean and the standard deviation of the signal.

Preprints (www.preprints.org) | NOT PEER-REVIEWED | Posted: 3 July 2020 doi:10.20944/preprints202007.0039.v1

Peer-reviewed version available at Biosensors 2020, 10, 89; doi:10.3390/bios10080089

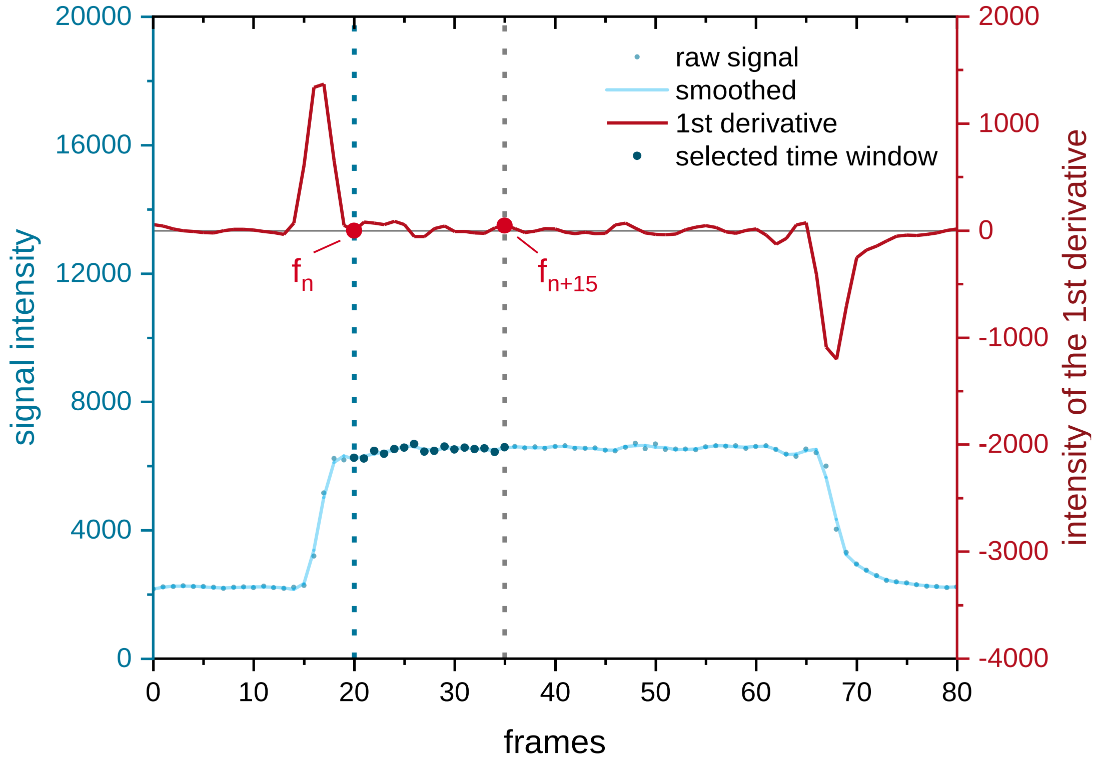

Figure 4. Determination of the first frame to be evaluated (f_n) based on the 1st derivative of the Savitzky–Golay-smoothed data shown for a sample injection of 100 pM Dy-654-COOH in PBS.

3.3. Antibody selection, validation, labeling, and determination of the test midpoint for TNT

The quality of an immunoassay is ultimately governed by the employed antibody. Thus, the antibody used must be chosen carefully with sensitivity and selectivity in mind. Many manufacturers only give an order number of an antibody. The properties or even the true clone identity may remain unclear [69]. This creates a risk for reliable and reproducible assays, which must not be tolerated when this information is critical. Two commercially available monoclonal anti-TNT antibodies A1.1.1 (SDIX, USA) and EW75C (BBI Solutions, UK) from mouse IgG_1 subclass were evaluated for their affinity to TNT for validation purposes. Also, their specific cross-reactivities with compounds of interest and high explosives (see Table T2 and Fig. S14, S15, SI) were determined. The clone A1.1.1 showed superior affinity by a factor of 30 (Fig. S16, SI) to the analyte TNT compared to the clone EW75C and was therefore chosen for this project. Additionally, for both clones, a mass spectrometric antibody fingerprint, according to Tscheuschner et al. [69] was generated (see Fig. S17, SI), which may be used to identify these clones in future work.

The sensor system relies on the sensitive detection of fluorophore-labeled antibodies in the eluate of the affinity column. A proper choice of fluorophore is, therefore, of considerable importance. A suitable label should display desirable properties like high quantum yield, high photostability, excellent water solubility, reduced aggregation, and low non-specific binding. Additionally, no detectable cross-reactivity with the antibody is imperative. Based on the available laser excitation source of 638 nm and excellent performance on epoxy functionalized glass substrates [70], the cyanine dye Dy-654 [Fig. 5] was chosen. The label features four sulfonic acids, which results in highly hydrophilic properties and minimal tendency for aggregation. Furthermore, the dye showed no detectable cross-reactivity with the antibody A1.1.1 in preliminary experiments.

Peer-reviewed version available at *Biosensors* **2020**, *10*, 89; doi:10.3390/bios10080089

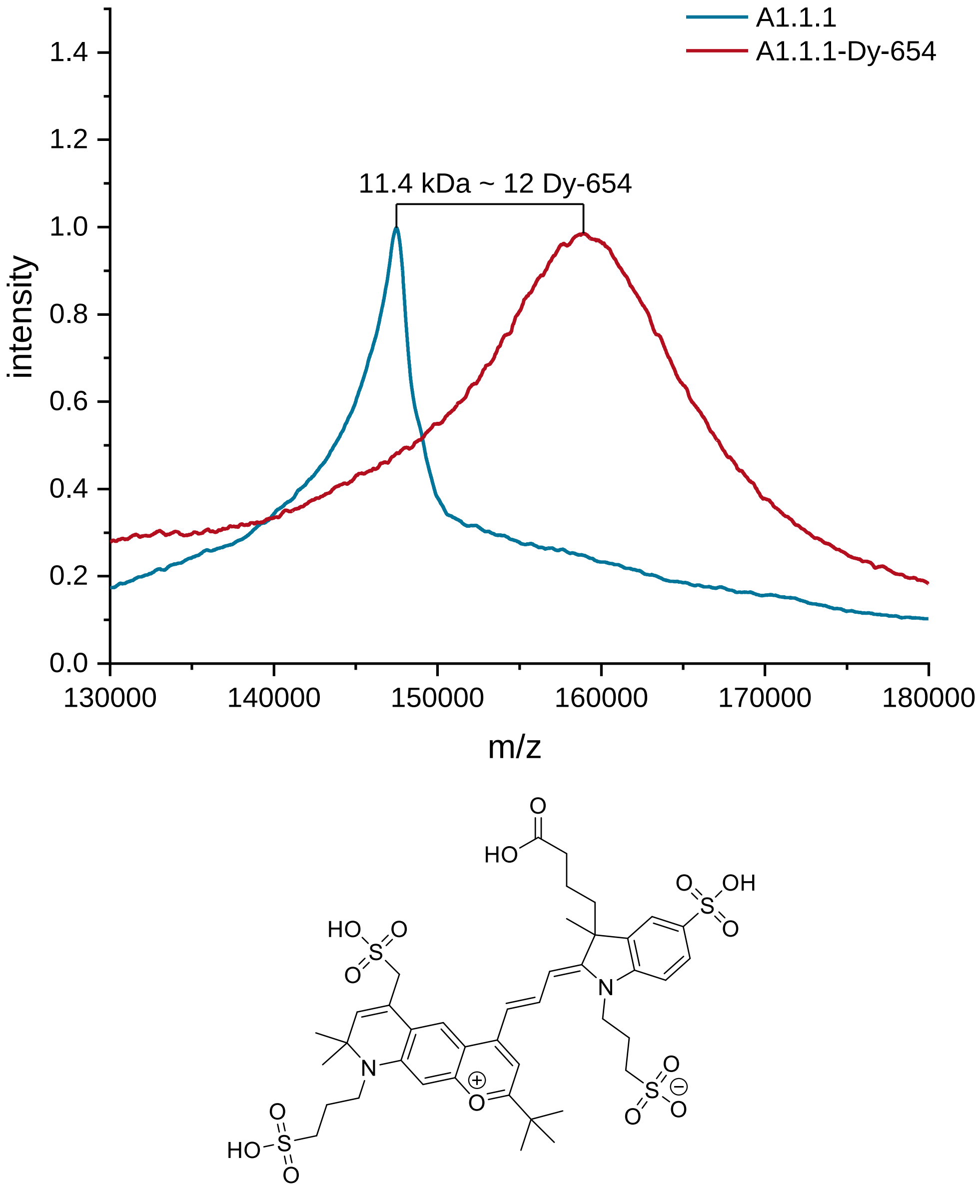

Figure 5. Smoothed MALDI-TOF MS spectra of the antibody A1.1.1 and the conjugate with Dy-654 (top) and structure of the label Dy-654-COOH (MW 1007.08 g/mol, Dyomics).

The degree of labeling (DOL) for the A1.1.1 Dy-654 conjugate was determined with MALDI-TOF MS to be approx. 12 (see Fig. 7) and the protein concentration of the A1.1.1 Dy-654 stock solution was determined to contain approx. 0.35 g/L antibody according to UV measurements. The test midpoint (IC_{50}) was determined by indirect competitive ELISA to be 1.2 nM (see Fig. 6), which is in excellent agreement with the literature stated value determined for the clone A1.1.1 of 1.3 nM [45]. The LOD on the indirect ELISA was determined to be approx. 170 pM.

Preprints (www.preprints.org) | NOT PEER-REVIEWED | Posted: 3 July 2020 doi:10.20944/preprints202007.0039.v1

Peer-reviewed version available at *Biosensors* **2020**, *10*, 89; doi:10.3390/bios10080089

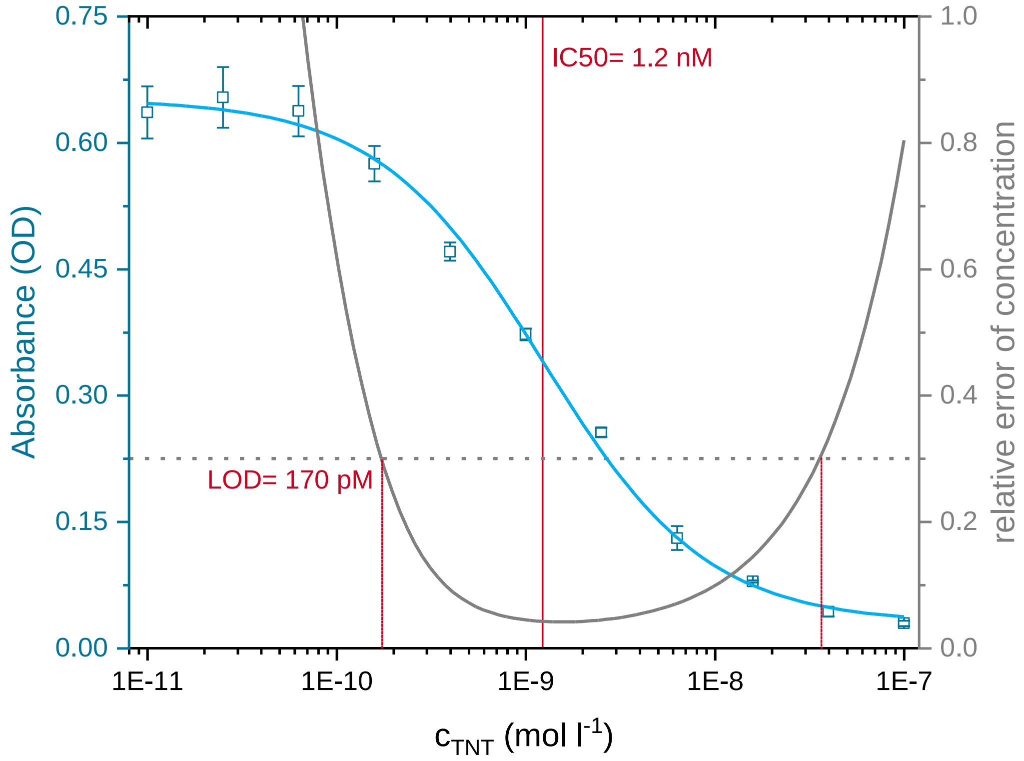

Figure 6. Precision profile of the chosen clone A1.1.1 determined by indirect ELISA with the analyte TNT as quadruplicates.

3.4. 2,4,6-Trinitrophenyl-(TNP)-BSA affinity columns

The degree of labeling of the BSA was determined by MALDI-TOF MS to be approximately 8 TNP molecules per BSA (see Fig. S2, SI). In preliminary tests, the TNP-BSA and the BSA column showed no non-specific interaction for the label Dy-654-COOH or Dy-654 labeled human IgG_1 (Avastin). The backpressure of a monolithic column was determined to be about 2.7 bar at a flow rate of 0.5 mL min^{-1} of PBS (see Fig. S3). The columns were stored under 80 % of ethanol in the fridge at 4 °C for several months without noticeable degradation of column performance.

3.5 Setup optimization and label LOD

The exposure time, the sensor gain, and the sensor temperature were varied to determine the optimal ratio of signal height and noise (S/N). To calculate the S/N, the signal difference between the signal intensity of 100 pM Dy-654-COOH dissolved in PBS and pure PBS was divided by the sum of the standard deviation of the Dy-654-COOH and the blank signal. The most substantial influence on the S/N was observed for the exposure time. Longer exposure times up to 5,000 ms and even beyond, increased the S/N (see Fig. S8). Increasing sensor gain reduced the S/N, especially at a gain > 4 (see Fig. S9). The temperature had no clear impact on S/N (see Fig. S10), as the known hot pixels were already removed by the python script. An exposure time of 5,000 ms and a gain of 4 was chosen to achieve a wide dynamic range and acceptable response times. The sensor temperature was set to -5°C, which was the lowest temperature the camera was able to keep over longer times at ambient temperatures around 25° C. These settings were applied in all measurements in this paper if not stated otherwise.

Solutions of Dy-654-COOH were prepared in PBS from 5 to 25 pM to determine the LOD and LOQ for the label and dilutions from 100 to 1000 pM to assess the range of the linear response (see

Fig. 9). After a stable signal was achieved, 16 frames were used to calculate the mean and standard deviation for each dilution step, as described above. The LOD and the LOQ were calculated by the addition of 3 or 10 times the standard deviation of the blank sample. For this setup, a LOD of about 1 pM was achieved for Dy-654-COOH. The dynamic range was about a factor of 250, ranging from at least 4 to 1000 pM. A highly linear response (Fig. 7) was achieved.

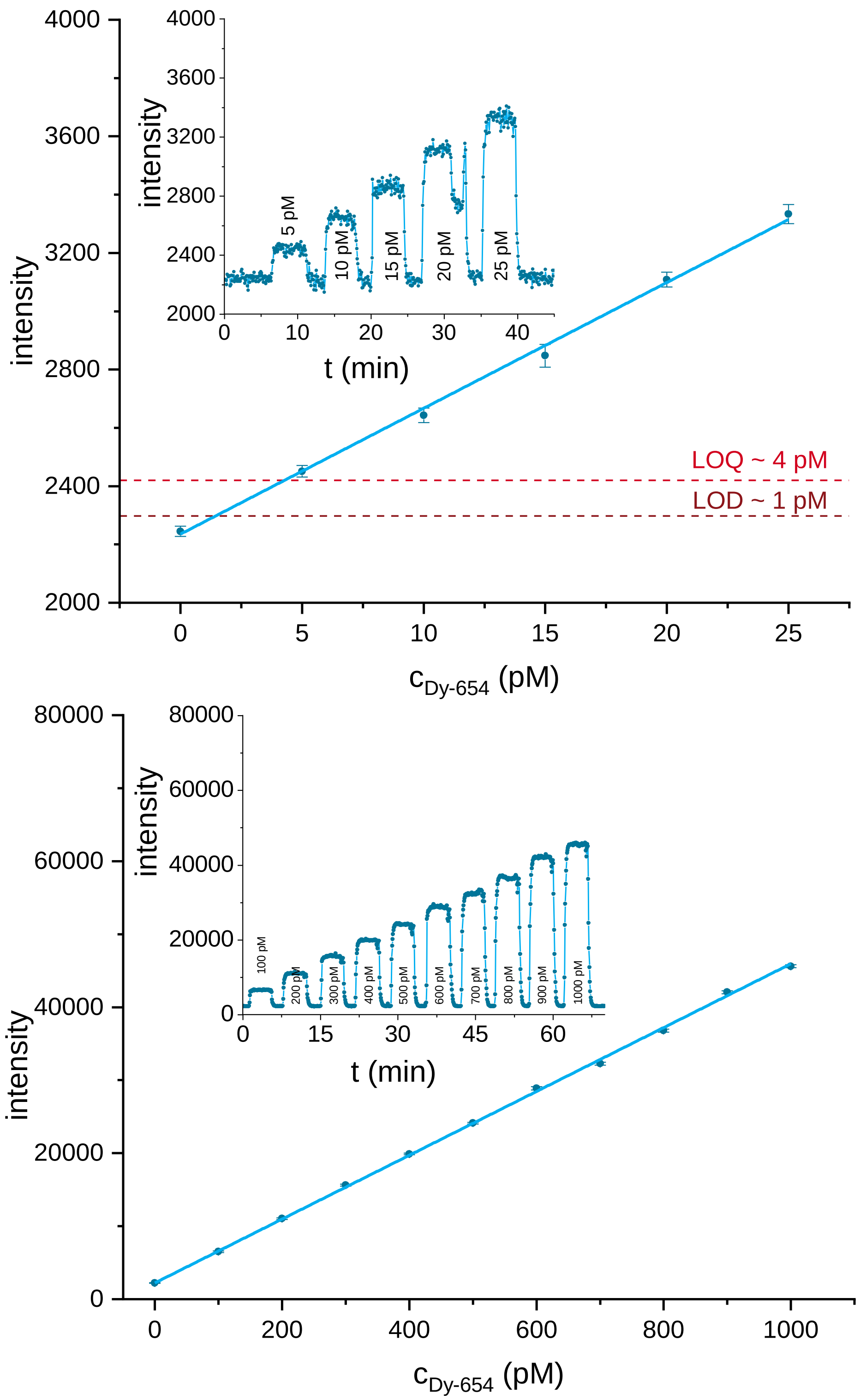

Figure 7. Determination of the LOD and LOQ (top) for the fluorescence label Dy-654-COOH and calibration line in the linear range from 4-1000 pM (bottom).

3.6 Performance of affinity column

Peer-reviewed version available at Biosensors 2020, 10, 89; doi:10.3390/bios10080089

To evaluate the performance of the TNP-BSA affinity column, a 1:100,000 dilution of the labeled antibody (≈ 3.5 µg/L) was injected onto the affinity column at varying flow rates, and the signal intensity of the eluate was monitored. At the lowest flow rate of 0.0625 mL min^{-1} the highest antibody retention of approx. 70% was observed. The antibody removal efficiency gradually declined until the highest flow rate of 0.5 mL min^{-1} was applied with approx. 54% retention (see. Fig. S11). When the dead volume of ca. 1 mL is considered (tubing, connectors, and the affinity column), a flow rate of 0.0625 mL min^{-1} would result in a dead time between injection and measurement of about 16 minutes. But this delay can be reduced to about 2 minutes if the highest flow rate of 0.5 mL min^{-1} would be applied. For all further measurements, a flow rate of 0.5 mL min^{-1} was used.

3.6. TNT measurements

Samples from 2 to 10 nM of TNT in 3.5 µg/L of antibody conjugate were incubated for five minutes and injected to determine the dynamic range for the analyte TNT. The results showed that the linear range does not extend well beyond 2 nM for the chosen parameters (see Fig. S12, SI). The signal displays an asymptotic behavior. In order to determine the LOD (3s) and LOQ (10s) of the biosensor, dilutions containing 0 to 1.0 nM TNT in 3.5 µg/L Dy-654-labeled A1.1.1 were incubated for five minutes and injected. The raw data were evaluated as described above. From 0 to 1.0 nM TNT, a linear response was observed, and the LOD and LOQ were determined to be about 0.1 nM or 20 ppt TNT and 0.4 nM or 90 ppt TNT, respectively (see Fig. 8).

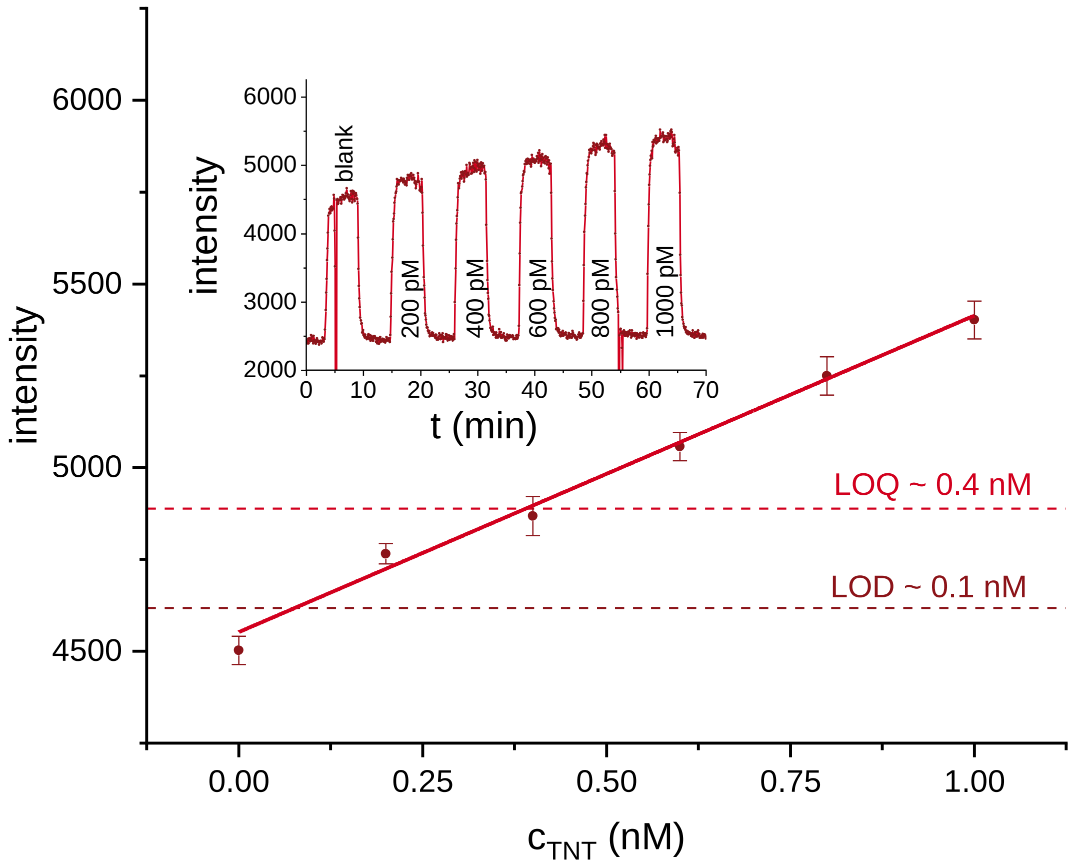

Figure 8. Biosensor measurements of TNT solutions in the range from 0 to 1 nM with a linear fit. LOD and LOQ were determined as 0.1 nM (20 ppt) and 0.4 nM (90 ppt). Error bars refer to the standard deviation. The biosensor signal is shown above.

Aqueous solutions of the common high explosives PETN, RDX, HMX, and TNT (5,000 pM) were incubated for five minutes with 3.5 µg/L of the labeled antibody and injected. No cross-reactivity

Peer-reviewed version available at Biosensors 2020, 10, 89; doi:10.3390/bios10080089

could be observed at 5,000 pM, for all explosives, except TNT (see Fig. 12). The results are in good agreement with the detailed characterization of the clone A1.1.1 (see Fig. S16 and Table T2) and the literature.

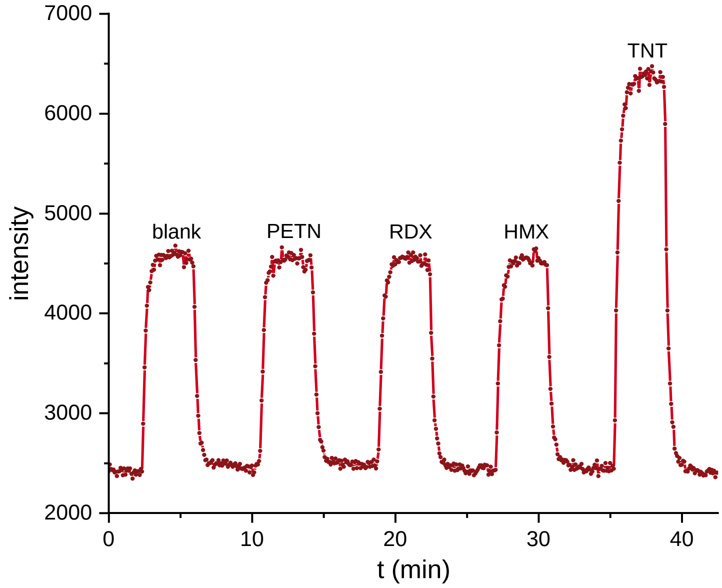

Figure 10. Biosensor-based cross-reactivity test for the high explosives PETN, RDX, HMX, and TNT at 5,000 pM. Only TNT shows a positive signal.

4. Discussion

In this paper, a sensitive and fast biosensor for the detection of 2,4,6-trinitrotoluene (TNT) at the ppt (ng/L or pM) level in water is presented. It is based on kinetic competition and hence displays some extraordinary properties. First of all, the biosensor is faster than most competitive immunoassays, which rely on the approximation to a solid-phase equilibrium. In our format, the analyte is incubated in a homogeneous solution with the respective antibody, which is a fast process. In addition, it is advantageous that this biosensor can be considered as quasi-continuous due to the very high capacity of the trapping column. This long-term measurement capability can even be extended by the regeneration of the trapping column, which, however, is not shown here. Another advantage is the calibration curve, which displays a positive slope in contrast to conventional competitive assays. There is a small delay of about two minutes between the analyte injection and the signal increase due to the dead volumes in the system. Shorter connections and higher flow rates could reduce this in the future.

Although the general setup of the system consisting of a wide-field epifluorescence system is quite common, one of the aims of the project was to establish a highly sensitive laser-induced fluorescence detector (LIF), with low-cost equipment (see Fig. S4, SI). For many applications, the budget is limited, and hence, systems based on expensive high-end components may not find broad application. Fortunately, the prices of many semiconductor devices, such as cooled CCD or CMOS cameras, dropped extremely, without compromising their performance.

Another decision is the choice of a suitable (fluorescence) label. During the last decades, many improved fluorescence dyes became commercially available, showing better quantum yield, ozone, bleaching and pH stability, less tendency for aggregation, water-solubility, ease of conjugation, and many more. Finally, we have chosen a highly hydrophilic dye, which can be exited with a wavelength of about 635 nm, for which small and cheap diode lasers are available.

One of the most critical and often neglected issues is the selection of the antibody. Only very few (monoclonal) antibodies against explosives or TNT, respectively, are available. We were able to

Preprints (www.preprints.org) | NOT PEER-REVIEWED | Posted: 3 July 2020 doi:10.20944/preprints202007.0039.v1

Peer-reviewed version available at Biosensors 2020, 10, 89; doi:10.3390/bios10080089

purchase two anti-TNT-antibodies, the clones A1.1.1 and EW75C. We have characterized both antibodies in detail to determine their sensitivity and their cross-reactivity patterns. In most cases, the cross-reactivities (CR) were relatively similar (see table T2, SI). Both clones displayed a high cross-reactivity against 2,4,6-trinitroaniline and a relatively high CR against 2,4,6-trinitrobenzene and some dinitrobenzenes or dinitrotoluenes. A significant difference is the lack of CR against any nitro musk compounds of the clone EW75C, in contrast to A1.1.1 (see Table T2). The opposite is the case with some nitrophenyl alkyl acids. The most relevant difference, however, is the test midpoint in ELISA format, which is around 1.2 nM (270 ng/L) for A1.1.1 and 36 nM (8.2 µg/L) for EW75C (see Fig. S17, SI). Due to this significant sensitivity difference, we have chosen to proceed with A1.1.1 only. For identification purposes for both clones, antibody fingerprints have been prepared, which are shown in the supplement (S18, SI).

Liquid handling is another issue in biosensor development. In our system, we rely on high-performance syringe pumps, which are robust and deliver a nearly pulsation-free flow. The sample and the antibody are premixed and injected with a conventional 6-port injection valve. A real sampling system for air or wipe tests is lacking, yet. The antibody trap is based on an in-house developed monolithic affinity column. It is manufactured from partially sintered borosilicate glass powder and coated via silane chemistry and conjugation with trinitrophenyl-derivatized albumin. The glass monolith is glued into a titanium shell and attached to standard HPLC fittings. These glass monoliths have the advantage that they tolerate high flow rates while displaying low backpressures and show fast binding kinetics due to a lack of internal porosity. As a miniaturized flow-cell, a microfluidic COC chip was used. This polymer shows excellent optical properties, which are similar to glass, and is resistant to most chemical attacks, as from acids and bases.

The optical system consists of a Zeiss objective for microscopes, a dichroic mirror, different filters, and a diode laser (635 nm, <1 mW). A cooled CMOS camera containing a Sony IMX-174M chip was used as the optical detector.

In total, the cost of this setup was about < 5000 EUR (incl. taxes, Table T2), which is quite moderate for this level of performance.

In order to characterize the system, several tests have been performed. First of all, the sensitivity of the detector was examined with dilutions of the fluorescence dye (Dy-654-COOH). A highly linear relationship was obtained in the concentration range of 0-1000 pM. A limit of detection (LOD) of about 1 pM was found (Fig. 7). In another experiment, the trapping efficiency of the affinity column was examined (Fig. S11, SI). An efficiency of 60-70% was achieved, which might indicate some conjugate impurities. Due to the shorter response time, the faster flow rate of 0.5 mL/min was chosen. In Fig. 8, the detection of TNT was tested with the setup shown in Fig. 2 and 3. A LOD of approx. 0.1 nM or 20 ppt TNT was obtained, which is significantly lower than the LOD of 60 ppt of a highly optimized competitive ELISA [45], and surpassing most biosensors based on the same antibody [4,26,30,31,38,71-84].

Finally, some basic cross-reactivity tests with high explosives have been performed with the new biosensor format. It could be shown that only TNT leads to a significant signal at 5,000 pM. PETN, RDX, and HMX did not show any increased signal even at much higher concentrations.

Conclusions

It could be shown that biosensors based on kinetic competition are very powerful and promising systems for the fast and highly sensitive detection of explosives, such as TNT. In contrast to many other biosensors presented for TNT and other nitroaromatic compounds, this approach does not depend on any specific physicochemical property of the target compound. It hence can be easily transferred to all other substances of interest, for which suitable monoclonal antibodies or similar binders can be made. High speed and excellent sensitivity are also striking advantages. Although these systems are highly specific and hence primarily designed for mono-analyte detection, the setup can be easily parallelized and therefore transformed into a multiplex biosensor system. Particularly the use of a conventional CMOS camera offers the opportunity to detect many signals in parallel

Peer-reviewed version available at *Biosensors* **2020**, *10*, 89; doi:10.3390/bios10080089

without the need for an additional detector or the use of highly expensive EMCCD cameras. Similarly, the beam of the laser diode might be split into several sub-beams to excite several flow channels on one chip at a time. Finally, it has to be stressed that due to the use of extraordinarily selective antibodies as binders, these biosensors are not prone to false-positive signals, which is crucial for any real-world application in the security field.

Supplementary Materials: The following are available online at www.mdpi.com/xxx/s1, Description of the semi-automated data evaluation.

Author Contributions: Experimental work, M.P., S.H., G.T; conceptualization, M.G.W.; methodology, M.P., and M.G.W.; software, M.P.; validation, M.P., and M.G.W.; resources, M.G.W; data curation, M.P.; writing—original draft preparation, M.G.W.; writing—review and editing, M.P. and M.G.W.; visualization, M.P.; project administration, M.G.W.; funding acquisition, M.G.W; experimental work, M.P., S.H., G.T.

Funding: This research received no external funding.

Acknowledgments:

We would like to thank Peter Taube for contributions for monolithic columns, Florian Weigert for the spectral characterization of the laser diode, Bettina Röder for the design and construction of the column holder, Melisa Kadem for laboratory experiments, Marco Wilke for the preparation and characterization of monolithic columns and finally the BAM division 2.3 for the delivery of explosives for the cross-reactivity testing.

Conflicts of Interest: The authors declare no conflict of interest.

References

1. Moore, D.S. Instrumentation for trace detection of high explosives. *Rev Sci Instrum* **2004**, *75*, 2499-2512, doi:10.1063/1.1771493.
2. Caygill, J.S.; Davis, F.; Higson, S.P.J. Current trends in explosive detection techniques. *Talanta* **2012**, *88*, 14-29, doi:10.1016/j.talanta.2011.11.043.
3. Brown, K.E.; Greenfield, M.T.; McGrane, S.D.; Moore, D.S. Advances in explosives analysis-part I: animal, chemical, ion, and mechanical methods. *Anal Bioanal Chem* **2016**, *408*, 35-47, doi:10.1007/s00216-015-9040-4.
4. Onodera, T.; Toko, K. Towards an Electronic Dog Nose: Surface Plasmon Resonance Immunosensor for Security and Safety. *Sensors-Basel* **2014**, *14*, 16586-16616, doi:10.3390/s140916586.
5. Ewing, R.G.; Atkinson, D.A.; Eiceman, G.A.; Ewing, G.J. A critical review of ion mobility spectrometry for the detection of explosives and explosive related compounds. *Talanta* **2001**, *54*, 515-529, doi: 10.1016/S0039-9140(00)00565-8.
6. Crawford, C.L.; Hill, H.H. Evaluation of false positive responses by mass spectrometry and ion mobility spectrometry for the detection of trace explosives in complex samples. *Anal Chim Acta* **2013**, *795*, 36-43, doi:10.1016/j.aca.2013.07.070.
7. Salinas, Y.; Martinez-Manez, R.; Marcos, M.D.; Sancenon, F.; Costero, A.M.; Parra, M.; Gil, S. Optical chemosensors and reagents to detect explosives. *Chem Soc Rev* **2012**, *41*, 1261-1296, doi:10.1039/c1cs15173h.
8. Lubczyk, D.; Siering, C.; Lorgen, J.; Shifrina, Z.B.; Mullen, M.; Waldvogel, S.R. Simple and sensitive online detection of triacetone triperoxide explosive. *Sensor Actuat B-Chem* **2010**, *143*, 561-566, doi:10.1016/j.snb.2009.09.061.
9. Lubczyk, D.; Grill, M.; Baumgarten, M.; Waldvogel, S.R.; Mullen, K. Scaffold-Optimized Dendrimers for the Detection of the Triacetone Triperoxide Explosive

Peer-reviewed version available at *Biosensors* **2020**, *10*, 89; doi:10.3390/bios10080089

Using Quartz Crystal Microbalances. *Chempluschem* **2012**, *77*, 102-105, doi:10.1002/cplu.201100080.

10. Kartha, K.K.; Babu, S.S.; Srinivasan, S.; Ajayaghosh, A. Attogram Sensing of Trinitrotoluene with a Self-Assembled Molecular Gelator. *J Am Chem Soc* **2012**, *134*, 4834-4841, doi:10.1021/ja210728c.
11. Yang, J.S.; Swager, T.M. Porous shape persistent fluorescent polymer films: An approach to TNT sensory materials. *J Am Chem Soc* **1998**, *120*, 5321-5322, doi: 10.1021/ja9742996.
12. Chang, C.P.; Chao, C.Y.; Huang, J.H.; Li, A.K.; Hsu, C.S.; Lin, M.S.; Hsieh, B.R.; Su, A.C. Fluorescent conjugated polymer films as TNT chemosensors. *Synthetic Met* **2004**, *144*, 297-301, doi:10.1016/j.synthmet.2004.04.003.
13. Tu, R.Y.; Liu, B.H.; Wang, Z.Y.; Gao, D.M.; Wang, F.; Fang, Q.L.; Zhang, Z.P. Amine-capped ZnS-Mn2+ nanocrystals for fluorescence detection of trace TNT explosive. *Anal Chem* **2008**, *80*, 3458-3465, doi:10.1021/ac800060f.
14. Fan, L.S.; Hu, Y.W.; Wang, X.; Zhang, L.L.; Li, F.H.; Han, D.X.; Li, Z.G.; Zhang, Q.X.; Wang, Z.X.; Niu, L. Fluorescence resonance energy transfer quenching at the surface of graphene quantum dots for ultrasensitive detection of TNT. *Talanta* **2012**, *101*, 192-197, doi:10.1016/j.talanta.2012.08.048.
15. Bhalla, V.; Pramanik, S.; Kumar, M. Cyanide modulated fluorescent supramolecular assembly of a hexaphenylbenzene derivative for detection of trinitrotoluene at the attogram level. *Chem Commun* **2013**, *49*, 895-897, doi:10.1039/c2cc36872b.
16. Yang, X.; Wang, J.H.; Su, D.Y.; Xia, Q.D.; Chai, F.; Wang, C.G.; Qu, F.Y. Fluorescent detection of TNT and 4-nitrophenol by BSA Au nanoclusters. *Dalton T* **2014**, *43*, 10057-10063, doi:10.1039/c4dt00490f.
17. Qian, J.J.; Qiu, L.G.; Wang, Y.M.; Yuan, Y.P.; Xie, A.J.; Shen, Y.H. Fabrication of magnetically separable fluorescent terbium-based MOF nanospheres for highly selective trace-level detection of TNT. *Dalton T* **2014**, *43*, 3978-3983, doi:10.1039/c3dt52777h.
18. Mandal, M.; Balamurugan, R. Efficient Sensing of Trinitrotoluene Using a Photoluminescent Benzo[a]fluorenone Derivative. *Chemistryselect* **2019**, *4*, 10164-10168, doi:10.1002/slct.201902639.
19. Meaney, M.S.; McGuffin, V.L. Luminescence-based methods for sensing and detection of explosives. *Anal Bioanal Chem* **2008**, *391*, 2557-2576, doi:10.1007/s00216-008-2194-6.
20. Smith, R.G.; D'Souza, N.; Nicklin, S. A review of biosensors and biologically-inspired systems for explosives detection. *Analyst* **2008**, *133*, 571-584, doi:10.1039/b717933m.
21. Komikawa, T.; Tanaka, M.; Yanai, K.; Johnson, B.R.G.; Critchley, K.; Onodera, T.; Evans, S.D.; Toko, K.; Okochi, M. A bioinspired peptide matrix for the detection of 2,4,6-trinitrotoluene (TNT). *Biosens Bioelectron* **2020**, *153*, 112030, doi:10.1016/j.bios.2020.112030.
22. Zarejousheghani, M.; Lorenz, W.; Vanninen, P.; Alizadeh, T.; Cammerer, M.; Borsdorf, H. Molecularly Imprinted Polymer Materials as Selective Recognition

Sorbents for Explosives: A Review. *Polymers-Basel* **2019**, *11*, doi:10.3390/polym11050888.

23. Guo, Z.Z.; Florea, A.; Cristea, C.; Bessueille, F.; Vocanson, F.; Goutaland, F.; Zhang, A.D.; Sandulescu, R.; Lagarde, F.; Jaffrezic-Renault, N. 1,3,5-Trinitrotoluene detection by a molecularly imprinted polymer sensor based on electropolymerization of a microporous-metal-organic framework. *Sensor Actuat B-Chem* **2015**, *207*, 960-966, doi:10.1016/j.snb.2014.06.137.
24. Trammell, S.A.; Melde, B.J.; Zabetakis, D.; Deschamps, J.R.; Dinderman, M.A.; Johnson, B.J.; Kusterbeck, A.W. Electrochemical detection of TNT with in-line pre-concentration using imprinted diethylbenzene-bridged periodic mesoporous organosilicas. *Sensor Actuat B-Chem* **2011**, *155*, 737-744, doi:10.1016/j.snb.2011.01.039.
25. Stringer, R.C.; Gangopadhyay, S.; Grant, S.A. Detection of Nitroaromatic Explosives Using a Fluorescent-Labeled Imprinted Polymer. *Anal Chem* **2010**, *82*, 4015-4019, doi:10.1021/ac902838c.
26. Goldman, E.R.; Anderson, G.P.; Lebedev, N.; Lingerfelt, B.M.; Winter, P.T.; Patterson, C.H.; Mauro, J.M. Analysis of aqueous 2,4,6-trinitrotoluene (TNT) using a fluorescent displacement immunoassay. *Anal Bioanal Chem* **2003**, *375*, 471-475, doi:10.1007/s00216-002-1713-0.
27. Charles, P.T.; Adams, A.A.; Howell, P.B.; Trammell, S.A.; Deschamps, J.R.; Kusterbeck, A.W. Fluorescence-based Sensing of 2,4,6-Trinitrotoluene (TNT) Using a Multi-channeled Poly(methyl methacrylate) (PMMA) Microimmunosensor. *Sensors-Basel* **2010**, *10*, 876-889, doi:10.3390/s100100876.
28. Charles, P.T.; Rangasammy, J.G.; Anderson, G.P.; Romanoski, T.C.; Kusterbeck, A.W. Microcapillary reversed-displacement immunosensor for trace level detection of TNT in seawater. *Anal Chim Acta* **2004**, *525*, 199-204, doi:10.1016/j.aca.2004.08.038.
29. Shankaran, D.R.; Gobi, K.V.; Sakai, T.; Matsumoto, K.; Toko, K.; Miura, N. Surface plasmon resonance immunosensor for highly sensitive detection of 2,4,6-trinitrotoluene. *Biosens Bioelectron* **2005**, *20*, 1750-1756, doi:10.1016/j.bios.2004.06.044.
30. Onodera, T.; Mizuta, Y.; Horikawa, K.; Singh, P.; Matsumoto, K.; Miura, N.; Toko, K. Displacement Immunosensor Based on Surface Plasmon Resonance for Rapid and Highly Sensitive Detection of 2,4,6-Trinitrotoluene. *Sensor Mater* **2011**, *23*, 39-52.
31. Green, T.M.; Charles, P.T.; Anderson, G.P. Detection of 2,4,6-trinitrotoluene in seawater using a reversed-displacement immunosensor. *Anal Biochem* **2002**, *310*, 36-41, doi:10.1016/S0003-2697(02)00288-9.
32. Kawaguchi, T.; Shankaran, D.R.; Kim, S.J.; Matsumoto, K.; Toko, K.; Miura, N. Surface plasmon resonance immunosensor using Au nanoparticle for detection of TNT. *Sensor Actuat B-Chem* **2008**, *133*, 467-472, doi:10.1016/j.snb.2008.03.005.
33. Whelan, J.P.; Kusterbeck, A.W.; Wemhoff, G.A.; Bredehorst, R.; Ligler, F.S. Continuous-Flow Immunosensor for Detection of Explosives. *Anal Chem* **1993**, *65*, 3561-3565, doi:DOI 10.1021/ac00072a005.

Peer-reviewed version available at *Biosensors* **2020**, *10*, 89; doi:10.3390/bios10080089

34. Goldman, E.R.; Anderson, G.P.; Tran, P.T.; Mattoussi, H.; Charles, P.T.; Mauro, J.M. Conjugation of luminescent quantum dots with antibodies using an engineered adaptor protein to provide new reagents for fluoroimmunoassays. *Anal Chem* **2002**, *74*, 841-847, doi:10.1021/ac010662m.
35. Bart, J.C.; Judd, L.L.; Kusterbeck, A.W. Environmental immunoassay for the explosive RDX using a fluorescent dye-labeled antigen and the continuous-flow immunosensor. *Sensor Actuat B-Chem* **1997**, *39*, 411-418, doi:10.1016/S0925-4005(97)80244-4.
36. Rabbany, S.Y.; Lane, W.J.; Marganski, W.A.; Kusterbeck, A.W.; Ligler, F.S. Trace detection of explosives using a membrane-based displacement immunoassay. *J Immunol Methods* **2000**, *246*, 69-77, doi:10.1016/S0022-1759(00)00301-X.
37. Mitchell, J. Small Molecule Immunosensing Using Surface Plasmon Resonance. *Sensors-Basel* **2010**, *10*, 7323-7346, doi:10.3390/s100807323.
38. Onodera, T.; Ishii, R.; Yatabe, R.; Toko, K. Development of Sensor Surfaces Using Poly-(N-vinylformamide) for Sensitive Detection of 2,4,6-Trinitrotoluene by Displacement Method on a Surface Plasmon Resonance Sensor. *Sensor Mater* **2016**, *28*, 209-218, doi: 10.18494/SAM.2016.1171
39. Climent, E.; Groninger, D.; Hecht, M.; Walter, M.A.; Martinez-Manez, R.; Weller, M.G.; Sancenon, F.; Amoros, P.; Rurack, K. Selective, Sensitive, and Rapid Analysis with Lateral-Flow Assays Based on Antibody-Gated Dye-Delivery Systems: The Example of Triacetone Triperoxide. *Chem-Eur J* **2013**, *19*, 4117-4122, doi:10.1002/chem.201300031.
40. Ho, M.Y.; D'Souza, N.; Migliorato, P. Electrochemical Aptamer-Based Sandwich Assays for the Detection of Explosives. *Anal Chem* **2012**, *84*, 4245-4247, doi:10.1021/ac300606n.
41. Kim, T.H.; Lee, B.Y.; Jaworski, J.; Yokoyama, K.; Chung, W.J.; Wang, E.; Hong, S.; Majumdar, A.; Lee, S.W. Selective and Sensitive TNT Sensors Using Biomimetic Polydiacetylene-Coated CNT-FETs. *Acs Nano* **2011**, *5*, 2824-2830, doi:10.1021/nn103324p.
42. Liu, J.L.; Zabetakis, D.; Acevedo-Velez, G.; Goldman, E.R.; Anderson, G.P. Comparison of an antibody and its recombinant derivative for the detection of the small molecule explosive 2,4,6-trinitrotoluene. *Anal Chim Acta* **2013**, *759*, 100-104, doi:10.1016/j.aca.2012.10.051.
43. Kramer, P.M.; Kremmer, E.; Weber, C.M.; Ciumasu, I.M.; Forster, S.; Kettrup, A.A. Development of new rat monoclonal antibodies with different selectivities and sensitivities for 2,4,6-trinitrotoluene (TNT) and other nitroaromatic compounds. *Anal Bioanal Chem* **2005**, *382*, 1919-1933, doi:10.1007/s00216-005-3294-1.
44. Charles, P.T.; Shriver-Lake, L.C.; Francesconi, S.C.; Churilla, A.M.; Rangasammy, J.G.; Patterson, C.H.; Deschamps, J.R.; Kusterbeck, A.W. Characterization and performance evaluation of in vivo and in vitro produced monoclonal anti-TNT antibodies for the detection of TNT. *J Immunol Methods* **2004**, *284*, 15-26, doi:10.1016/j.jim.2003.09.010.

Peer-reviewed version available at *Biosensors* **2020**, *10*, 89; doi:10.3390/bios10080089

45. Zeck, A.; Weller, M.G.; Niessner, R. Characterization of a monoclonal TNT-antibody by measurement of the cross-reactivities of nitroaromatic compounds. *Fresen J Anal Chem* **1999**, *364*, 113-120, doi:10.1007/s002160051309.
46. Julicher, P.; Mussenbrock, E.; Renneberg, R.; Cammann, K. Broadening the Antibody Specificity by Hapten Design for an Enzyme-Linked Immunoassay as an Improved Screening Method for the Determination of Nitroaromatic Residues in Soils. *Anal Chim Acta* **1995**, *315*, 279-287, doi:Doi 10.1016/0003-2670(95)00318-T.
47. Hesse, A.; Biyikal, M.; Rurack, K.; Weller, M.G. Development of highly sensitive and selective antibodies for the detection of the explosive pentaerythritol tetranitrate (PETN) by bioisosteric replacement. *J Mol Recognit* **2016**, *29*, 88-94, doi:10.1002/jmr.2511.
48. Ramin, S.; Weller, M.G. Extremely sensitive and selective antibodies against the explosive 2,4,6-trinitrotoluene by rational design of a structurally optimized hapten. *J Mol Recognit* **2012**, *25*, 89-97, doi:10.1002/jmr.2162.
49. Walter, M.A.; Pfeifer, D.; Kraus, W.; Emmerling, F.; Schneider, R.J.; Panne, U.; Weller, M.G. Triacetone Triperoxide (TATP): Hapten Design and Development of Antibodies. *Langmuir* **2010**, *26*, 15418-15423, doi:10.1021/la1018339.
50. Walter, M.A.; Panne, U.; Weller, M.G. A Novel Immunoreagent for the Specific and Sensitive Detection of the Explosive Triacetone Triperoxide (TATP). *Biosensors (Basel)* **2011**, *1*, 93-106, doi:10.3390/bios1030093.
51. Anderson, G.P.; Goldman, E.R. TNT detection using llama antibodies and a two-step competitive fluid array immunoassay. *J Immunol Methods* **2008**, *339*, 47-54, doi:10.1016/j.jim.2008.08.001.
52. Ulaeto, D.O.; Hutchinson, A.P.; Nicklin, S. Sub-Nanogram Detection of RDX Explosive by Monoclonal Antibodies. *Monoclon Antib Immunodiagn Immunother* **2015**, *34*, 225-227, doi:10.1089/mab.2015.0010.
53. Freytag, J.W.; Dickinson, J.C.; Tseng, S.Y. A Highly Sensitive Affinity-Column-Mediated Immunometric Assay, as Exemplified by Digoxin. *Clin Chem* **1984**, *30*, 417-420.
54. Freytag, J.W.; Lau, H.P.; Wadsley, J.J. Affinity-Column-Mediated Immunoenzymometric Assays - Influence of Affinity-Column Ligand and Valency of Antibody Enzyme Conjugates. *Clin Chem* **1984**, *30*, 1494-1498.
55. Leflar, C.C.; Freytag, J.W.; Powell, L.M.; Strahan, J.C.; Wadsley, J.J.; Tyler, C.A.; Miller, W.K. An Automated, Affinity-Column-Mediated, Enzyme-Linked Immunometric Assay for Digoxin on the Du-Pont Aca Discrete Clinical Analyzer. *Clin Chem* **1984**, *30*, 1809-1811.
56. Bauer, C.G.; Eremenko, A.V.; Kuhn, A.; Kurzinger, K.; Makower, A.; Scheller, F.W. Automated amplified flow immunoassay for cocaine. *Anal Chem* **1998**, *70*, 4624-4630, doi:10.1021/ac971388s.
57. Weller, M.G. Immunochromatographic techniques - a critical review. *Fresen J Anal Chem* **2000**, *366*, 635-645, doi:10.1007/s002160051558.
58. Oosterkamp, A.J.; Irth, H.; Herraiz, M.T.V.; Tjaden, U.R.; vanderGreef, J. Theoretical concepts of on-line liquid chromatographic biochemical detection

systems .1. Detection systems based on labelled ligands. *J Chromatogr A* **1997**, *787*, 27-35, doi:10.1016/S0021-9673(97)00646-8.

59. Oosterkamp, A.J.; Irth, H.; Tjaden, U.R.; vanderGreef, J. Theoretical concepts of on-line liquid chromatographic biochemical detection systems .2. Detection systems based on labelled affinity proteins. *J Chromatogr A* **1997**, *787*, 37-46, doi:10.1016/S0021-9673(97)89244-8.
60. Gunaratna, P.C.; Wilson, G.S. Noncompetitive Flow-Injection Immunoassay for a Hapten, Alpha-(Difluoromethyl)Ornithine. *Anal Chem* **1993**, *65*, 1152-1157, doi:10.1021/ac00057a009.
61. Hafner, F.T.; Kautz, R.A.; Iverson, B.L.; Tim, R.C.; Karger, B.L. Noncompetitive immunoassay of small analytes at the femtomolar level by affinity probe capillary electrophoresis: Direct analysis of digoxin using a uniform-labeled scFv immunoreagent. *Anal Chem* **2000**, *72*, 5779-5786, doi:DOI 10.1021/ac000853+.
62. Fintschenko, Y.; Wilson, G.S. Flow injection immunoassays: a review. *Mikrochim Acta* **1998**, *129*, 7-18, doi:10.1007/Bf01246843.
63. Oates, M.R.; Clarke, W.; Zimlich, A.; Hage, D.S. Optimization and development of a high-performance liquid chromatography-based one-site immunometric assay with chemiluminescence detection. *Anal Chim Acta* **2002**, *470*, 37-50, doi:10.1016/S0003-2670(02)00302-1.
64. Pfaunmiller, E.L.; Anguizola, J.A.; Milanuk, M.L.; Papastavros, E.; Carter, N.; Matsuda, R.; Zheng, X.W.; Hage, D.S. Development of microcolumn-based one-site immunometric assays for protein biomarkers. *J Chromatogr A* **2014**, *1366*, 92-100, doi:10.1016/j.chroma.2014.09.026.
65. Lovgren, U.; Kronkvist, K.; Backstrom, B.; Edholm, L.E.; Johansson, G. Design of non-competitive flow injection enzyme immunoassays for determination of haptens: application to digoxigenin. *J Immunol Methods* **1997**, *208*, 159-168, doi: 10.1016/S0022-1759(97)00144-0.
66. Danilova, N.P.; Beckman, N.I.; Yazynin, S.A.; Vasilov, R.G. Fast Filtration Enzyme-Immunoassay for Haptens. *Immunol Lett* **1992**, *33*, 157-162, doi:Doi 10.1016/0165-2478(92)90041-L.
67. Ohmura, N.; Lackie, S.J.; Saiki, H. An immunoassay for small analytes with theoretical detection limits. *Anal Chem* **2001**, *73*, 3392-3399, doi:10.1021/ac001328d.
68. Blake, R.C.; Pavlov, A.R.; Blake, D.A. Automated kinetic exclusion assays to quantify protein binding interactions in homogeneous solution. *Anal Biochem* **1999**, *272*, 123-134, doi:10.1006/abio.1999.4176.
69. Tscheuschner, G.; Schwaar, T.; Weller, M.G. Fast Confirmation of Antibody Identity by MALDI-TOF MS Fingerprints. *Antibodies (Basel)* **2020**, *9*, doi:10.3390/antib9020008.
70. Paul, M.; Weller, M.G. Antibody Screening by Microarray Technology-Direct Identification of Selective High-Affinity Clones. *Antibodies (Basel)* **2020**, *9*, doi:10.3390/antib9010001.

Peer-reviewed version available at *Biosensors* **2020**, *10*, 89; doi:10.3390/bios10080089

71. Sapsford, K.E.; Charles, P.T.; Patterson, C.H.; Ligler, F.S. Demonstration of four immunoassay formats using the array biosensor. *Anal Chem* **2002**, *74*, 1061-1068, doi:10.1021/ac0157268.
72. Bromberg, A.; Mathies, R.A. Homogeneous immunoassay for detection of TNT and its analogues on a microfabricated capillary electrophoresis chip. *Anal Chem* **2003**, *75*, 1188-1195, doi:10.1021/ac020599g.
73. Bromberg, A.; Mathies, R.A. Multichannel homogeneous immunoassay for detection of 2,4,6-trinitrotoluene (TNT) using a microfabricated capillary array electrophoresis chip. *Electrophoresis* **2004**, *25*, 1895-1900, doi:10.1002/elps.200305818.
74. Anderson, G.P.; Moreira, S.C.; Charles, P.T.; Medintz, I.L.; Goldman, E.R.; Zeinali, M.; Taitt, C.R. TNT detection using multiplexed liquid array displacement immunoassays. *Anal Chem* **2006**, *78*, 2279-2285, doi:10.1021/ac051995c.
75. Kawaguchi, T.; Shankaran, D.R.; Kim, S.J.; Gobi, K.V.; Matsumoto, K.; Toko, K.; Miura, N. Fabrication of a novel immunosensor using functionalized self-assembled monolayer for trace level detection of TNT by surface plasmon resonance. *Talanta* **2007**, *72*, 554-560, doi:10.1016/j.talanta.2006.11.020.
76. Shankaran, D.R.; Kawaguchi, T.; Kim, S.J.; Matsumoto, K.; Toko, K.; Miura, N. Evaluation of the molecular recognition of monoclonal and polyclonal antibodies for sensitive detection of 2,4,6-trinitrotoluene (TNT) by indirect competitive surface plasmon resonance immunoassay. *Anal Bioanal Chem* **2006**, *386*, 1313-1320, doi:10.1007/s00216-006-0699-4.
77. Anderson, G.P.; Lamar, J.D.; Charles, P.T. Development of a luminex based competitive immunoassay for 2,4,6-trinitrotoluene (TNT). *Environ Sci Technol* **2007**, *41*, 2888-2893, doi:10.1021/es062333n.
78. Girotti, S.; Eremin, S.A.; Montoya, A.; Moreno, M.J.; Caputo, P.; D'Elia, M.; Ripani, L.; Romolo, F.S.; Maiolini, E. Development of a chemiluminescent ELISA and a colloidal gold-based LFIA for TNT detection. *Anal Bioanal Chem* **2010**, *396*, 687-695, doi:10.1007/s00216-009-3264-0.
79. Giannetto, M.; Maiolini, E.; Ferri, E.N.; Girotti, S.; Mori, G.; Careri, M. Competitive amperometric immunosensor based on covalent linking of a protein conjugate to dendrimer-functionalised nanogold substrate for the determination of 2,4,6-trinitrotoluene. *Anal Bioanal Chem* **2013**, *405*, 737-743, doi:10.1007/s00216-012-6137-x.
80. Wang, J.; AlMakhaita, M.; Biswal, S.L.; Segatori, L. Sensitive Detection of TNT using Competition Assay on Quartz Crystal Microbalance. *J. Biosens. Bioelectron.* **2012**, *3*, 1-7, doi:10.4172/2155-6210.1000115.
81. Charles, P.T.; Wadhwa, V.; Kouyate, A.; Mesa-Donado, K.J.; Adams, A.A.; Deschamps, J.R.; Kusterbeck, A.W. A High Aspect Ratio Bifurcated 128-Microchannel Microfluidic Device for Environmental Monitoring of Explosives. *Sensors-Basel* **2018**, *18*, doi:10.3390/s18051568.
82. Yatabe, R.; Onodera, T.; Toko, K. Fabrication of an SPR Sensor Surface with Antifouling Properties for Highly Sensitive Detection of 2,4,6-Trinitrotoluene Using Surface-Initiated Atom Transfer Polymerization. *Sensors-Basel* **2013**, *13*, 9294-9304, doi:10.3390/s130709294.

83. Mizuta, Y.; Onodera, T.; Singh, P.; Matsumoto, K.; Miura, N.; Toko, K. Development of an oligo(ethylene glycol)-based SPR immunosensor for TNT detection. *Biosens Bioelectron* **2008**, *24*, 191-197, doi:10.1016/j.bios.2008.03.042.
84. Singh, P.; Onodera, T.; Mizuta, Y.; Matsumoto, K.; Miura, N.; Toko, K. Novel DNP-KLH protein conjugate surface for sensitive detection of TNT on SPR immunosensor. *Sensor Mater* **2007**, *19*, 261-273.